Identification of near-fault multi-pulse ground motion

Guan Chen[a,b], Yong Liu[a,*] and Michael Beer[b,c,d]

[a] State Key Laboratory of Water Resources and Hydropower Engineering Science, Institute of Engineering Risk and Disaster Prevention, Wuhan University, Wuhan 430072, PR China

[b] Institute for Risk and Reliability, Leibniz Universität Hannover, 30167 Hannover, Germany

[c] Institute for Risk and Uncertainty and School of Engineering, University of Liverpool, Liverpool L69 72F, UK

[d] International Joint Research Center for Resilient Infrastructure & International Joint Research Center for Engineering Reliability and Stochastic Mechanics, Tongji University, Shanghai 200092, PR China

ARTICLE INFO

Keywords:
Multi-Pulse ground motion
Near-source earthquake
Convolution analysis
Pulse-like ground motion
Continuous wavelet transform

Abstract

The near-fault pulse-like ground motion is of practical importance since it tends to cause severer damage to structures than ordinary ground motion in engineering and helps characterize the seismic source and the kinematic characteristics of the geological fault in seismology. However, previous investigations mainly focus on single-pulse ground motion. As one of the particular seismic records in the near-fault earthquake, the multi-pulse ground motion is rarely considered caused by the absence of an effective identification method. Hence, a generalized continuous wavelet transform (GCWT) method is proposed by combining convolution analysis with evaluation parameters to facilitate wider studies on multi-pulse ground motion. In identification, the proposed method requires each pulse in the multi-pulse ground motion to satisfy the same criteria and excludes the effects of attenuation component. In methodology, the proposed method overcomes the limitations of the classical CWT method that requires a wavelet basis and provides a workable and flexible framework for pulse-like ground motion identification. Based on the method, single- and multi-pulse ground motions from two typical near-fault earthquakes on the PEER NGA-West2 database were identified. The effects of the pulse model and ground motion orientation on identification are discussed. Besides, the 5% damped spectral velocity of multi-pulse ground motions potentially contain multiple peaks in the high-period range. This phenomenon implies that the risk would be underestimated for the response spectrum-based seismic hazards and risk analysis if the multi-pulse features are not, or are insufficiently taken into account.

1. Introduction

The near-fault pulse-like ground motions, which feature long period and high amplitude in velocity, have attracted increasing attention since it was reported in the 1960s [1]. The pulse-like ground motion is significant because it potentially causes severer damage on structures than ordinary ground motions (e.g., [2–4]) and helps reveal the seismic source and kinematic characteristics of geological fault (e.g., [5, 6]). However, previous studies mainly focused on single-pulse ground motions. The multi-pulse ground motion is rarely considered even though it exists in records and is verified to potentially cause severer damage to structures than single-pulse ground motions by artificial simple signals, like triangle wave, square wave, and harmonic wave [7–9]. Hence, this study attempts to propose a multi-pulse ground motion identification method to facilitate wider studies on multi-pulse records. A generalized continuous wavelet transform (GCWT) method by combining convolution analysis with evaluation parameters is proposed, which requires each pulse in the multi-pulse ground motion to satisfy the same criteria. Besides, It can identify the multi-pulse

*Corresponding author

guan.chen@irz.uni-hannover.de (G. Chen); liuy203@whu.edu.cn (Y. Liu); beer@irz.uni-hannover.de (M. Beer)

ORCID(s):

ground motions and corresponding parameters (such as Peak Ground Velocity (PGV), pulse period, pulse location, and the number of pulses) and overcome the limitation of the wavelet transform that requires a wavelet basis. Compared with the black-box methods, the proposed method provides a workable and flexible framework, which enables adding or deleting other processing procedures or supplementary criteria. The identification of multi-pulse ground motion can also help determine critical scenarios for seismic demand analysis in near-fault regions and provide new insights for inverting the seismological parameters.

Some efforts on multi-pulse ground motion identification have been made. For example, Lu et al. [10] proposed a wavelet-based iteration scheme to identify the multi-pulse ground motions. Chen et al. [11, 12] identified the multiple pulses based on the Hilbert-Huang transform and analyzed the multi-pulse characteristics on the number of inherent pulses together with the pulse periods, amplitudes, and the timing of each pulse. However, in contrast to the single-pulse ground motion identification that the CWT-based method proposed by Baker [13] is widely accepted, the evaluation standards and identification method for multi-pulse ground motion are still in debate. Hence, this study aims to propose a novel method, which features each pulse in the multi-pulse ground motion satisfying the same criteria and excludes the influences of attenuation component that includes in most other methods. To propose an effective multi-pulse ground motion identification method, Table 1 briefly summarizes the main-stream methods in pulse-like ground motion identification.

Table 1 shows that two factors are critical for pulse-like ground motion identification, that is, the pulse model and evaluation parameters. The former determines the shape of the extracted pulse, and the latter classifies the pulse and non-pulse ground motion. Many investigations on the pulse model were carried out to accurately extract the pulse. For example, Mavroeidis and Papageorgiou [14] proposed a mathematical pulse model and calibrated it with plenty of recorded ground motions. Bray and Rodriguez-Marek [15] analyzed the characteristics of pulse-like ground motion caused by the forward directivity effects and proposed empirical parameterization relationships for estimating PGV, pulse periods, and the number of pulses. The wavelet basis is also widely applied as the pulse model [13, 16, 17] since the great resolutions of wavelet transform on both time- and frequency- domain [18]. Besides, some studies directly adopted the half-cycles of the original ground motion as the pulse [19]. These methods effectively avoid the selection of a pulse model, but some limitations exist. Specifically, (i) these pulse-like ground motion methods mainly focus on signal processing and cannot consider seismological parameters. (ii) The shape of the identified pulse is easily affected by noise and interference. For example, when the recorded ground motion contains complex high-frequency components, these components are also part of the identified pulse.

The evaluation parameters in pulse-like ground motion identification mainly include the ratio between the PGV and Peak Ground Acceleration (PGA), pseudo-velocity response spectrum, and the energy ratio between the pulse part and the whole ground motion. The PGV/PGA ratio is often applied to analyze the frequency characteristics of pulse-like

Table 1
Brief summary of pulse-like ground motion identification methods.

References	Method	Pulse model	Evaluation parameters
Liu et al. 2020 [20]	Relative energy zero ratio-based method	No model, using the pulses in original ground motions	Energy ratio of pulse-like ground motion
Zhai et al. 2018 [19]	Significant velocity half-cycles	No model, using the pulses in original ground motions	Energy ratio of half-cycle
Zhao et al. 2016 [21]	Zero Velocity Point Method (ZVPM)	No model, using sine wave fitting the pulse	Energy ratio of vibration interval defined by ZVPM
Mimoglou et al. 2014 [22]	Response spectrum-based method	M&P wavelet	Cumulative absolute displacement; Product spectrum of velocity and displacement response spectra
Mukhopadhyay and Gupta 2013 [23]	Energy-based method	Mexican Hat function, Integral of the Mexican hat function	Energy ratio of half-cycle
Zhai et al. 2013 [24]	Energy-based method	Mathematical model [17]	Energy ratio of pulse-like ground motion
Baker 2007 [13]	Continuous wavelet transform	'db4' wavelet	Both the PGV ratio and energy ratio between the original and residual ground motions
Loh et al. 2001 [25]	EMD and Hilbert spectrum method	No model, the pulse constructed by the IMF components	Absolute energy of cumulative IMF that decomposed by Empirical Model Decomposition (EMD)

ground motions. For example, Malhotra [26] think that the pulse-like ground motions are the low-frequency signals if the PGV/PGA ratio is greater than 0.16. Since the pulse period needs to be directly identified, the PGV/PGA ratio is not used in this study. The corresponding period of the maximum pseudo-velocity response spectrum value is regarded as the pulse period sometimes [27]. However, the accuracy of this method may be not desirable [13]. To further clarify the relationship between the pulse period and the pseudo-velocity response spectrum, a careful discussion is conducted in Section 5. Compared with these two parameters, the energy ratio between the pulse part and the whole ground motion has been widely validated on detecting the pulse-like ground motion [23, 24]. Therefore, the energy ratio is adopted to distinguish pulse and non-pulse in this study. Besides, a new parameter, the Pearson correlation coefficient between the recorded pulse part and the pulse model, is introduced in this study. The correlation coefficient is utilized for two reasons: (i) evaluating the applicability of the adopted pulse model and (ii) avoiding the effects of trend terms on pulse-like ground motion identification.

Owing to the theoretical equivalence between the continuous wavelet transform and convolution analysis [28] and the successful applications of the continuous wavelet transform in pulse velocity identification [13], the GCWT method by combining convolution analysis and evaluation parameters (i.e., energy ratio and correlation coefficient) is proposed. This study requires each pulse in the identified multi-pulse ground motion to satisfy the same criteria. The pulse-like ground motions from Imperial Valley-06 Earthquake and the Taiwan Chi-Chi Earthquake at the Pacific Earthquake Engineering Research (PEER) Center NGA-West2 are identified based on the proposed method. The

identification results and corresponding parameters are listed in Appendix at Table 3 to facilitate further studies on multi-pulse ground motion. The pulse period among the proposed method, the Baker's method [13], and Zhai et al. [24] is compared to verify the proposed method. The effects of the pulse model on identification are carefully discussed. The pseudo-spectral velocity of multi-pulse ground motion is also analyzed. The successful identification of multi-pulse ground motions would provide seismologists and earthquake engineers new insight, such as ground motion simulation, earthquake dynamics, and seismic damage analysis.

This study is organized as follows: the mechanism of convolution analysis in pulse-like ground motion identification, the step-by-step procedures of the proposed method, and the cons and pros between the proposed method and classical CWT method are explained in Section 2. In Section 3, examples are illustrated the proposed method in single- and multi-pulse ground motion identification. In Section 4, the pulse-like ground motions in the Imperial Valley-06 earthquake and Chi-Chi Taiwan earthquake are identified and are summarized in Appendix at Table 3. The advantages and limitations of the proposed method are also highlighted. The effects of the pulse model and orientation on identification, together with the pseudo spectral velocity characteristics of multi-pulse ground motions, are discussed in Section 5. The main conclusions are drawn in Section 6.

2. Methodology

2.1. Pulse detection using convolution analysis

For a discrete-time ground motion V_s and pulse model $\omega(T_p)$, the convolution W can be expressed in Eq. (1).

$$W(k) = \sum_j u(j)v(k-j+1), (1 \leqslant k \leqslant m_p + n - 1, k \in \mathbb{Z}^+) \tag{1}$$

where $V_s = [v(1), v(2), v(3), ..., v(n)]$ (n is the length of the original ground motions); $\omega(T_p) = [u(1), u(2), u(3), ..., u(m_p)]$ (m_p is the length of the pulse model, which is related to the pulse period T_p); j is the serial number of data, its satisfying $max(1, m+1-n) \leqslant j \leqslant min(k, m_p), (j \in \mathbb{Z}^+)$; the length of W is $(m_p + n - 1)$; the time interval of W is $1/f_s$, where f_s is the sampling frequency of the original ground motion.

From the perspective of signal processing, the convolution can be regarded as a Linear Time-Invariant (LTI) system, where $\omega(T_p)$ is the unit impulse response; V_s is the input signal, and W is the output signal. Algebraically, W is the integral of products between the 'unit' of the input signal and the unit impulse response. As the unit impulse response is confirmed (i.e., pulse model in this study), the value of W can reflect two characteristics of the 'unit' of the input signal, that is, the amplitude and the shape. Moreover, the absolute value of W increases with the amplitude value and the similarity in shape between the unit impulse response and the 'unit' of the input signal. Hence, the maximum absolute value of W is obtained when the 'unit' of the input signal contains the local peak amplitude and is similar

to the period of the unit impulse response. In other words, the maximum absolute convolution result is obtained when the identified pulse contains the local PGV and is similar to the period of the pulse model. The PGV and period are the core parameters of pulse-like ground motion. Therefore, the maximum absolute value of convolution is feasible for locating the pulse-like ground motion.

After the potential pulse is detected, the evaluation parameter (energy ratio and correlation coefficient) are applied to judge pulse and non-pulse. A step-by-step procedure of the proposed method is explained in the next section.

2.2. Step-by-step Procedures

The flowchart of the proposed method is shown in Figure 1. A step-by-step outline of the proposed procedure is explained as follows.

Step 1: Setting the velocity threshold value V_{thre}. Containing a larger PGV is one of the most critical and straightforward criteria for pulse-like ground motions. Hence, selecting a proper threshold velocity value V_{thre} is the initial step. This value may differ for different purposes. This study recommends 30 cm/s from the view of seismic damage analysis [8, 13].

$$max(abs(V_s)) > V_{thre} \tag{2}$$

where $max(abs(V_s))$ means the maximum absolute value of original ground motion.

Step 2: Selecting and resampling the pulse model and calculating the convolution between the resampled pulse model and input ground motion. An appropriate pulse model is significant since the shape of the extracted pulse mainly depends on the pulse model. Many relevant studies have been carried out to characterize the pulse [23, 24]. To extract different periods of pulse-like ground motion, the pulse model needs to be resampled. The duration of the resampled pulse model ω' should satisfy Eq. (3). The time interval of the resampled pulse model needs to agree with the original ground motion, i.e., equaling $1/f_s$ (f_s is the sampling frequency of the original ground motion). The convolution between the original ground motion and the resampled pulse model is calculated using Eq. (1).

$$t_p = \frac{T_p}{T_0} \cdot t_0 \tag{3}$$

where t_p is the duration of the resampled pulse model; t_0 is the duration of the original pulse model; T_p is the pulse period; T_0 is the period of the original pulse model.

Step 3: Extracting the pulse part in seismic records and scaling the pulse model. The formula for extracting the recorded pulse part is proposed in Eq. (4). Since the length of the resampled pulse model may be greater than that of the original ground motion, and the maximum absolute convolution results may locate in the negative of the x-axis (an example is shown in Figure 3(e)), the pulse model needs to be trimmed. The formula for updating the pulse model is

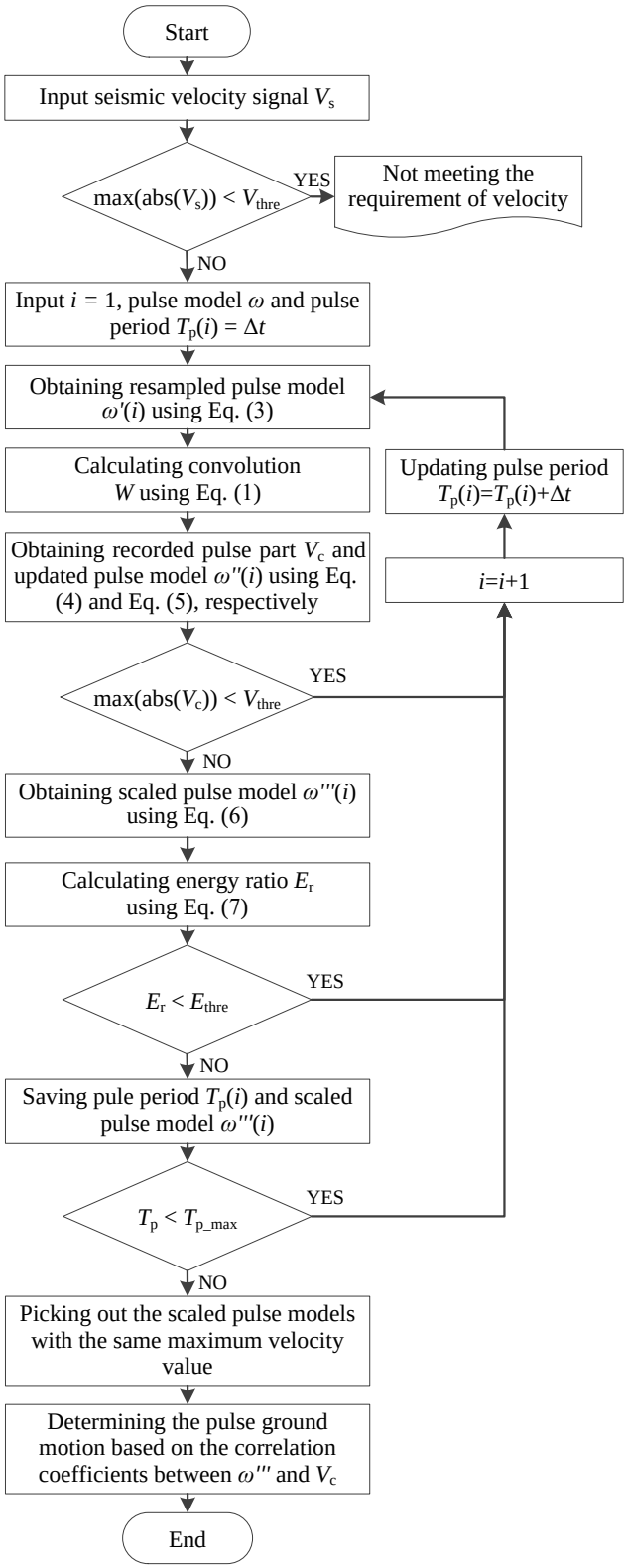

Figure 1: Flowchart of the proposed method.

shown in Eq. (5). Eq. (6) is applied to scale the updated pulse model to ensure the maximum value of the pulse model agrees with that of the ground motion.

$$V_c = V_s(a), (max(1, c_{max} - m_p + 1) \leqslant a \leqslant min(c_{max}, n), a \in \mathbb{Z}^+) \tag{4}$$

$$\omega'' = \omega'(b), (max(1, c_{max} - n + 1) \leqslant a \leqslant min(c_{max}, m_p), b \in \mathbb{Z}^+) \tag{5}$$

$$\omega''' = \frac{max(abs(V_c)}{max(abs(\omega))} \cdot \omega'' \tag{6}$$

where V_c is the recorded pulse part extracted by the proposed method; V_s is the original ground motion; a is the data series of the original ground motions; b is the data series of the resampled pulse model; c_{max} is the location of the maximum absolute value of the vector W; n is the length of the original ground motion; m_p is the length of resampled pulse model; ω is the original pulse model; ω' is the resampled pulse model using Eq. (3); ω'' is the updated pulse model using Eq. (5); ω''' is the scaled pulse model using Eq. (6) (ω, ω', ω'' and ω''' are illustrated in Figure 2(b)); $max(abs(V_c))$ and $max(abs(\omega))$ are the maximum absolute value of the original pulse model and recorded pulse part, respectively.

Step 4: Excluding the recorded pulse part using energy ratio. An energy ratio threshold E_{thre} is set to exclude the false identification of the pulse-like ground motion. The energy ratio is calculated by Eq. (7). When E_r is greater than E_{thre}, the pulse period T_p and the scaled pulse model ω''' are saved and adopted in subsequent steps.

$$E_r = \frac{\int_0^{t_p} V_c^2 \mathrm{d}t}{\int_0^t V_s^2 \mathrm{d}t} \tag{7}$$

where V_c is the recorded pulse part extracted by the proposed method; t_p is the duration of the identified pulse; V_s is the original ground motion; t is the duration of original ground motions.

Repeating Step 2 - Step 4 with $T_p = T_p + \Delta t$ (Δt is the pulse period interval) until T_p is greater than the set maximum pulse period T_{p_max}.

Step 5: Determining the pulse-like ground motion. Only one pulse should exist for one local peak velocity. However, different scaled pulse models may be around the same local peak velocity. Initially, all scaled pulse models that contain the same maximum absolute value but with different pulse periods are picked out. Subsequently, the correlation coefficients between the scaled pulse model and the corresponding recorded pulse part are calculated. The threshold value is also set for the correlation coefficient to exclude the pulses that may meet the energy requirements but not the pulse-like ground motion. The scaled pulse model with the maximum correlation coefficient and greater than the threshold is deemed as the extracted pulse eventually. Except for excluding the false identification of pulse-like ground

motion, the correlation coefficients can effectively reflect the similarity between the pulse model and the recorded pulse part, which is beneficial for evaluating the applicability of the pulse model.

2.3. Comparison with the CWT method

Currently, the most popular method in single-pulse ground motion identification is the CWT-based method proposed by Baker in 2007 [13]. To better understand the proposed method, the similarity and differences between the proposed method and Baker's method are clarified. The expression of continuous wavelet transform is shown in Eq. (8).

$$W f(u,s) = \int_{-\infty}^{+\infty} f(t) \frac{1}{\sqrt{s}} \psi^*(\frac{t-u}{s}) \mathrm{d}t, (u,s \in \mathbb{R}) \tag{8}$$

where $W f(u,s)$ is the continuous wavelet transform; $f(t)$ is the inputting signal; $\psi(t)$ is the wavelet basis; $\psi^*(t)$ represents the conjugate of $\psi(t)$; u and s denote the translation and scale parameter, respectively.

The convolution $(f * \psi_{u,s})(t)$ of inputting signal $f(t)$ and wavelet function $\psi_{u,s}(t)$ can be expressed as Eq. (9).

$$(f * \psi_{u,s})(t) = \left\langle f(t), \psi_{u,s}(t) \right\rangle = \int f(\tau) \cdot \psi^*(\frac{\tau-u}{s}) \mathrm{d}\tau \tag{9}$$

As shown in Eqs. (8) and (9), the theoretical essence between CWT and convolution analysis is equivalence. However, the proposed method contains several advantages compared with the classical CWT method. (1) The convolution analysis is not limited by the wavelet basis that the CWT requires. That is, any pulse model can be applied in the proposed method to identify the pulse-like ground motion. This property provides a manner to combine the proposed method with the seismology for pulse-like ground motion identification, like adopting a pulse model that can reflect the seismological characteristics of the earthquake. (2) In contrast to the black-box calculation procedures of the CWT method, the proposed method provides a workable and flexible framework that can adjust the analysis parameters. (3) The proposed method can identify the multi-pulse ground motions.

3. Illustrations

3.1. Pulse model selection and resample

The wavelet basis 'db4' is selected as the pulse model referring to Baker's study [13]. However, to reduce the effects of low amplitude at both ends, the wavelet basis is trimmed. Only the main part of the wavelet basis is kept. The original wavelet basis 'db4' and the selected pulse model are shown in Figure 2(a). The central frequency of the wavelet basis 'db4' is regarded as the frequency of the pulse model [13], which is about 0.71 Hz, and the corresponding period is 1.4 s. The cosine function with the frequency equalling 0.71 Hz is also plotted in Figure 2(a).

The pulse model is resampled using Eq. (3). Based on the characteristics of the original ground motions and the requirements of accuracy, the maximum pulse period T_{p_max} and the time interval Δt is set to 16 s and 0.1 s in this study, respectively. The sampling frequency of the pulse model is consistent with that of the original ground motion. After pulse models with different periods are obtained, they are applied to conduct convolution analysis with the original ground motion. To clarify the states of the pulse model in different steps, an example of the original, resampled, updated and scaled pulse model is shown in Figure 2(b).

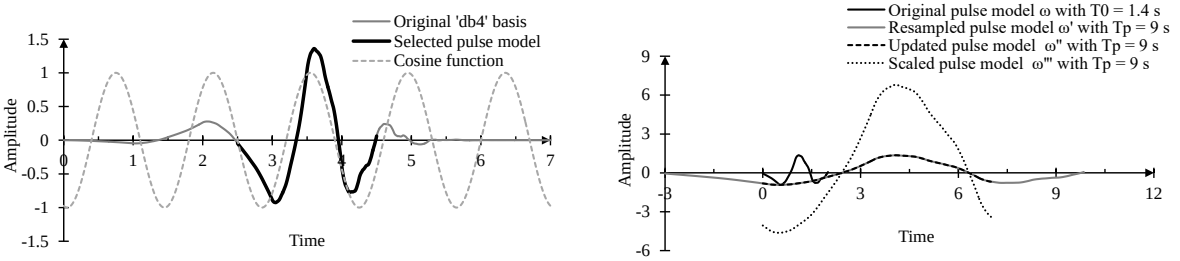

(a) (b)

Figure 2: The selected pulse model in this study. (a) Selected 'db4' pulse model. The period T_0 of this model is 1.4 s. (b) The original, resampled, updated and scaled pulse model. The pulse model needs to be updated as its length may be greater than that of the original ground motion and the maximum absolute convolution results may locate in the negative of x-axis.

3.2. Convolution analysis and pulse-like ground motion determination

The convolution analysis between the original ground motion and the resampled pulse model is performed using the RSN 158 Horizontal 1 in PEER NGA-West2 database as an example. As explained in Eqs. (1), (4), (5), and (6), both the scaled pulse model and the recorded pulse part can be obtained based on the maximum absolute value of convolution results. The pulse search and identification process of the proposed method, including original ground motion, convolution results, pulse model, and recorded pulse parts are illustrated in Figure 3. To present all results in one graph, the convolution results are scaled. The results indicate that the maximum absolute convolution result can locate the potential pulse-like ground motion effectively.

After the convolution analysis, the energy ratio between the recorded pulse parts and the original ground motion in different pulse periods are calculated using Eq. (7). Then, the threshold of energy ratio is applied to exclude the scaled pulse model that cannot meet the requirement of energy. Based on the study of Zhai et al. [24], the energy ratio of the pulse should be greater than 0.3. In this study, the threshold of energy ratio is also set to 0.3 after tests. Thereafter, the correlation coefficients between the recorded pulse parts and the corresponding scaled pulse models are calculated. The threshold value of the correlation coefficient is set to 0.6 after tests. The correlation coefficient would contain multiple peaks for the multi-pulse ground motion since it has multiple local peak values. Hence, the scaled pulse models with

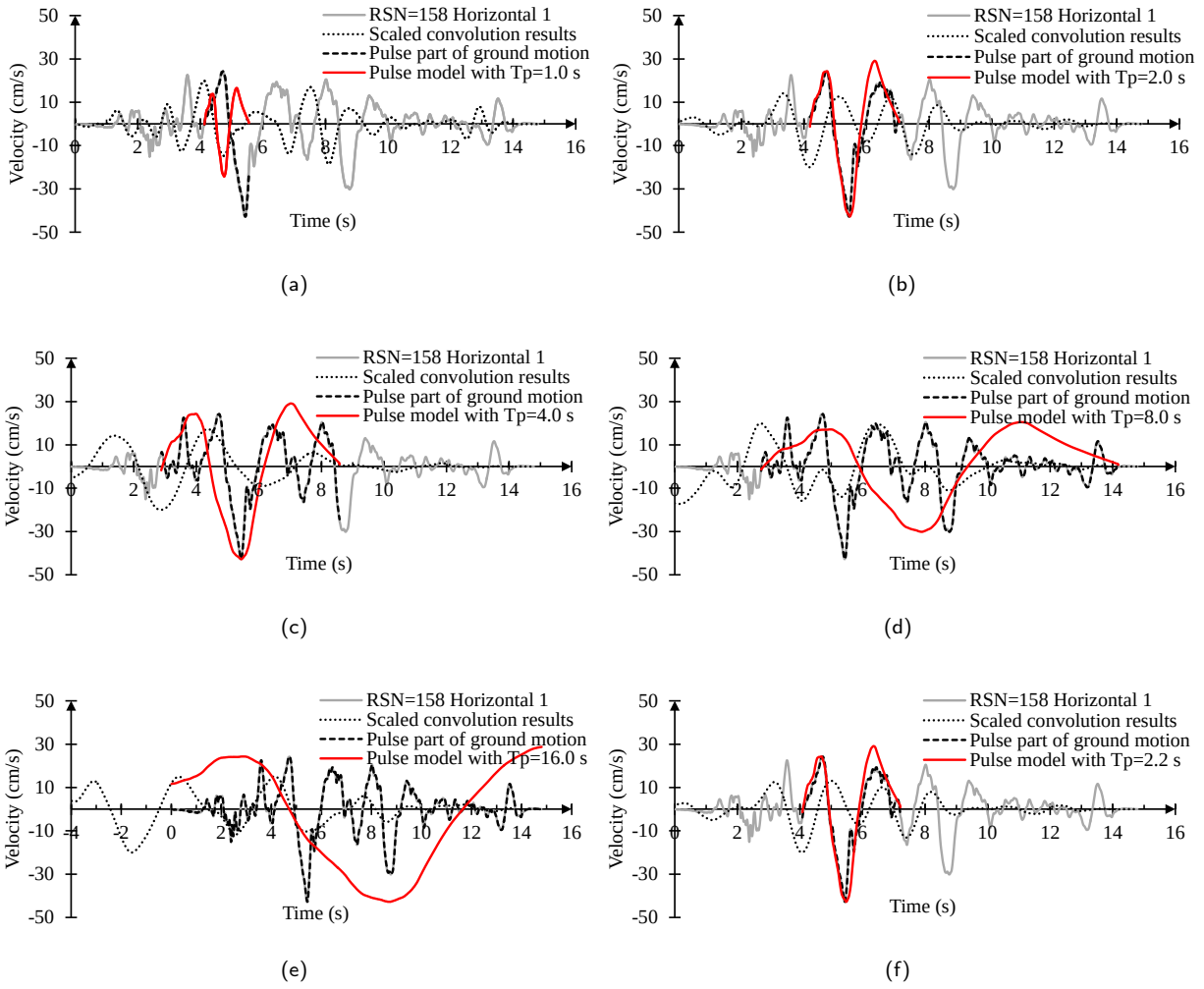

Figure 3: Pulse search and identification process of the proposed method. (a) - (e) are the cases excluded by evaluation parameters of the proposed method. (f) is the final identified pulse. Convolution analyses between the original ground motions and the resampled pulse models with pulse period (T_p) equal to (a) 1.0 s, (b) 2.0 s, (c) 4.0 s, (d) 8.0 s, (e) 16.0 s and (f) 2.2 s. (e) shows that the maximum absolute convolution result is located in the negative of x-axis, and the length of the pulse model is longer than that of the original ground motions. Hence, the pulse model needs to be trimmed based on Eq. (5) to match the original ground motion. When T_p is 1.0 s, 2.0 s, 4.0 s, 8.0 s, 16.0 s and 2.2 s, the corresponding correlation coefficients between the pulse model and the recorded pulse part are $-0.59, 0.94, 0.48, 0.07, 0.03$ and 0.96, respectively. Hence, the pulse model with period $T_p = 2.2s$ is regarded as the pulse in original ground motion without considering the requirement of energy. RSN is the Record Sequence Number in the PEER NGA-West2 flatfile. Horizontal 1 is the direction defined in the PEER NGA-West2 flatfile.

the same maximum value need to be picked out firstly. Then, the scaled pulse model with the maximum correlation coefficient and greater than 0.6 is regarded as the pulse.

Based on the proposed procedure, examples of single- and multi-pulse ground motions are identified. The original ground motion, convolution analysis, extracted pulse and recorded pulse part of ground motions from the Imperial Valley-06 Earthquake are shown in Figure 4. The examples of single- and multi-pulse-like ground motions

identification from the Chi-Chi, Taiwan Earthquake databases are shown in Figure 5. Figures 4 and 5 show that the proposed method can effectively identify both single- and multi-pulse-like ground motions.

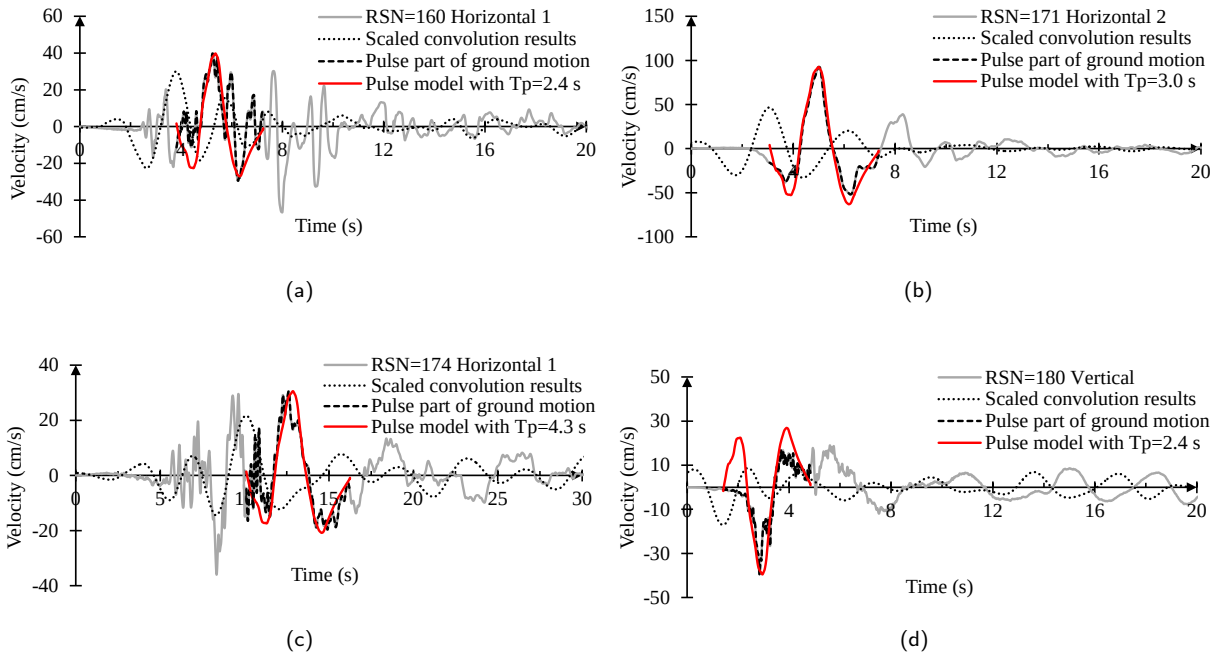

Figure 4: Examples of pulse-like ground motions identified by the proposed method in the Imperial Valley-06 Earthquake. (a) The ground motion is identified as non-pulse velocity in Baker's study, but identified as pulse-like ground motion in this study; (b) The pulse period of the proposed method is basically consistent with that of Baker's method; (c) The pulse periods are various between Baker's and Zhai et al.'s method; (d) The pulse-like ground motion in the vertical direction.

4. Results

Pulse-like ground motions from two typical near-fault earthquakes (Imperial Valley-06 Earthquake and Chi-Chi, Taiwan Earthquake) in the PEER NGA-West2 database are identified based on the proposed method. The required parameters and values of the proposed method are listed in Table 2. Since this study aims to propose a feasible method to identify the pulse-like ground motion rather than analyze the causes of the pulse-like ground motions, the originally ground motions in PEER at three different directions are identified. The identification results and corresponding parameters are summarized in Appendix.

The identification accuracy and calculation speed of the proposes method are elaborated. As one of the most critical parameters for pulse-like ground motions, the pulse period is usually utilized to verify pulse-like ground motion identification results. Currently, Baker's [13] and Zhai et al.'s [24] pulse period results are widely applied in single-pulse ground motions. Hence, a comparative study among the proposed and the existing approaches is carried out to verify the proposed method. Because the fault-normal (i.e. the strike-normal) ground motions are applied in Baker's

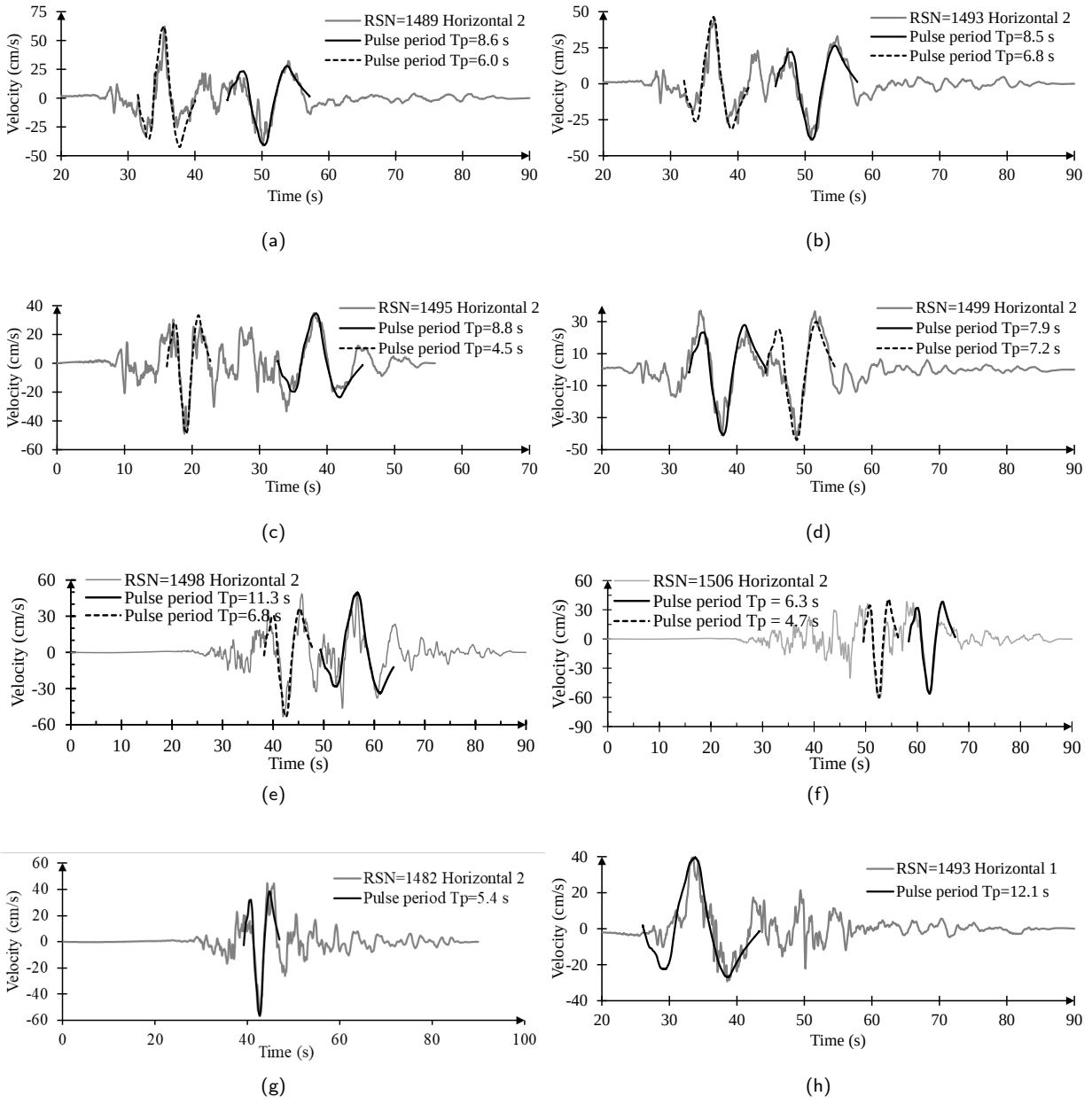

Figure 5: Examples of single- and multi-pulse ground motions identified by the proposed method in the Chi-Chi, Taiwan Earthquake. (a) - (f) are the multi-pulse ground motions; (g) is the ground motion identified as non-pulse in Baker's method; (h) is the case that agree well with Baker's method.

and Zhai et al.'s study, the ground motions are initially rotated into the fault-normal and fault-parallel orientation based on the azimuth of fault strike, Horizontal 1 and Horizontal 2 [29, 30]. Subsequently, the pulse parameters (including pulse period, Peak Ground Velocity (PGV), energy ratio, and correlation coefficient) on fault-normal and fault-parallel orientation are obtained based on the proposed method. The details are summarized in the Supplementary Information in Table S1. The quantitative comparison of pulse period among the proposed, Baker's and Zhai et al.'s methods in

Table 2
Parameters of the proposed methods used in this study.

Parameters	Sign	Value
Velocity threshold	V_{thre}	30 cm/s
Pulse model	ω	Trimmed 'db4'
Threshold of energy ratio	E_{thre}	0.3
Correlation coefficient threshold	ρ_{thre}	0.6
Pulse period interval	Δt	0.1 s
Maximum pulse period	T_{p_max}	16 s

the fault-normal orientation (see Figure 6) indicates that the pulse periods detected by the proposed method agree well with that of existing methods for the single-pulse ground motions. Specifically, the pulse periods among the three methods are basically distributed in the fluctuation range of $[-30\%, +30\%]$. Hence, the proposed method is workable for pulse-like ground motion identification.

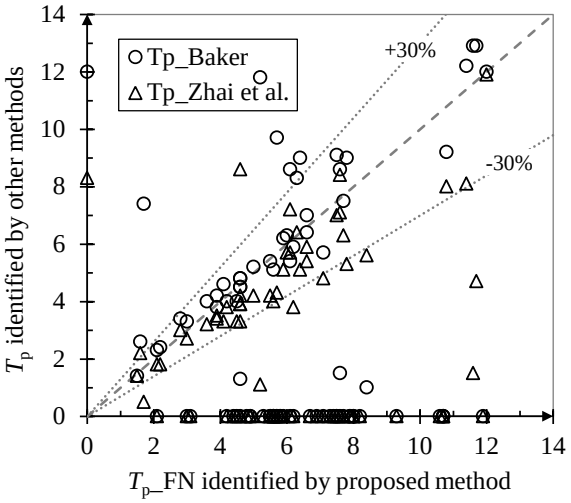

Figure 6: Pulse period (T_p) comparison among the proposed, Baker's [13] and Zhai et al.'s [24] methods in the fault-normal orientation. The symbol located in the axis coordinate indicates that the ground motion is identified as non-pulse ground motion in the other method.

Since the procedure only refers to basic mathematical calculation, the computational complexity is small. About 2 seconds are taken in Matlab for judging the pulse and non-pulse for each ground motion using PC with Intel 7 and SSD 500GB. Hence, the proposed procedure is effective and efficient.

The advantages and limitations of the proposed method are also highlighted. (i) The proposed method can effectively identify both single- and multi-pulse ground motions. Moreover, compared with previous identification methods in multi-pulse ground motion, the proposed method features each pulse in multi-pulse records satisfying the same criteria in Section 2.2 and excludes the effects of signal attenuation part that included in other methods. (ii) The introduced correlation coefficient can reflect the applicability of the adopted pulse model. It helps analyze

the effects of the pulse model on pulse-like ground motion identification. (iii) The proposed method can detect the critical parameters of pulse-like ground motion, including the pulse period, PGV, pulse location, and the number of pulses, which are beneficial for mathematically analyzing the characteristics of the pulse-like ground motions. The corresponding recorded pulse part can also be obtained, which often contains the high-frequency components and helps analyze the seismological characteristics of near-fault regions. (iv) The proposed method provides a feasible framework for pulse-like ground motion identification. Other processing procedures or supplementary criteria can be flexibly added into the proposed method, like adding criteria to exclude the late-arriving pulse-like ground motion. Especially, the proposed method is feasible for any pulse models, which provides a way to combine the proposed method with the seismology in pulse-like ground motion identification.

Some limitations also exist. The physical mechanisms of earthquake engineering and seismology are not considered. Besides, the extracted pulse may partially reflect the characteristics of the original pulse-like ground motion due to the limitations of the pulse model.

5. Discussions

5.1. Pulse model

The pulse model is critical in pulse-like ground motion identification as it directly determines the shape of the pulse. This study uses the wavelet basis 'db4' because it was also adopted in the study of Baker [13] and the pulse period in Baker was collected in the widely used PEER database. However, the 'db4' pulse model has some limitations. It cannot reflect the pulse shape of all identified pulse-like ground motions. An example of a real pulse-like record is shown in Figure 7.

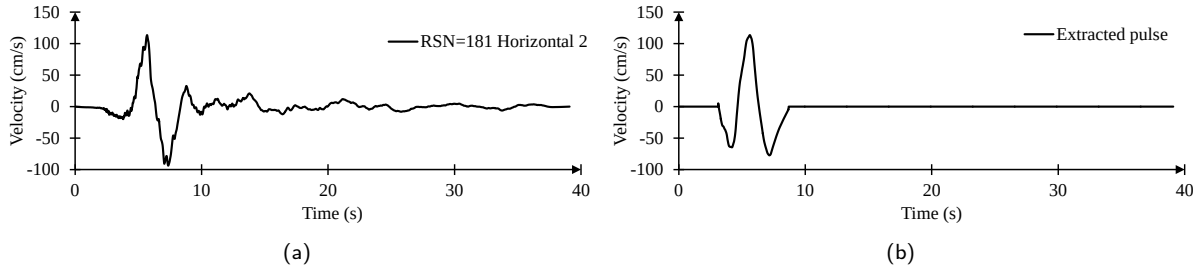

Figure 7: Example of the extracted pulse that just partially reflects the characteristics of recorded pulse part due to the limitation of 'db4' pulse model.

However, the proposed method is workable for any pulse model. This property provides a chance to mitigate the matching problem between the pulse-like ground motion and the pulse model by a seismological pulse model. An ideal seismological pulse model should satisfy two conditions. (i) The shape and the pulse period of the pulse model should be adjustable to fit the characteristics of different pulse-like ground motions. (ii) The seismological

pulse model needs to reflect the physical characteristics of the earthquake (including seismic source, propagation path and site characteristics). Some efforts on this issue have been made. Mavroeidis and Papageorgiou [14] proposed a mathematical pulse model based on various ground-motion records. Scala et al. [31] investigated that the emergence of pulse-like ground velocity is mainly related to the average value of the rise-time, site characteristics, rupture speed, and event depth. Mukhopadhyay and Gupta [32] proposed the relationships between the pulse parameters (including pulse amplitude, period, and location) and the seismological parameters to characterize the pulse model. However, further research needs to be conducted to obtain a more generalized seismological pulse model.

5.2. Ground motion orientations

The pulse-like ground motions are related to the fault rupture direction [33, 34]. For example, the pulse-like ground motions caused by the directivity effects and the fling step effects generally appear in the fault-normal and fault-parallel orientation, respectively [35, 36]. Hence, the fault-normal ground motions are usually adopted in analyzing the pulse-like ground motions caused by the directivity effects [13, 24]. However, owing to the influences of propagation path and site topographic feature (such as the basin-edge effect [37]), a strict correspondence between the occurrence orientation and the causes of pulse-like ground motions is not manifested. Zhai et al. [24] analyzed the effects of orientation on the pulse-like ground motion by rotating it to different azimuths. It shows that the pulse-like ground motion may not exist in fault-normal orientation even as the conditions of directivity effects are favourable. Besides, the fault-normal pulse-like ground motions may be not caused by directivity effects.

This study identifies the pulse-like ground motions in arbitrary orientation instead of analyzing the causes of pulse-like ground motion. Hence, the pulse-like ground motions caused by the forward directivity effects and the fling step effects are not classified. Moreover, to be consistent with the PEER ground motion database, three orientations in the PEER flatfiles are directly analyzed. The results (summarized in the Supplementary Information) show that the pulse-like ground motion also exists in the vertical direction; however, the occurrence possibility is much less than that of the horizontal direction.

To further discuss the effects of orientation on pulse-like ground motion occurrences, the pulse periods in fault-normal, fault-parallel, Horizontal 1, and Horizontal 2 orientations are compared. The results (see Figure 8) indicate that the pulse periods show a certain correlation as the pulse occurs in different directions simultaneously; however, the pulse-like ground motion occurrences are indeed associated with the ground motion orientation. Therefore, although a strict correspondence between the occurrence orientation and the causes is not manifested, the orientation should be considered in analyzing the causes of pulse-like ground motions.

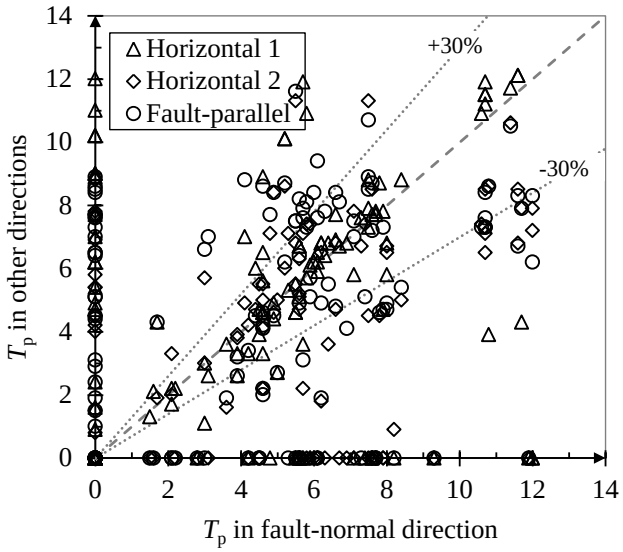

Figure 8: Pulse period comparison among the fault-normal, fault-parallel, Horizontal 1 and Horizontal 2 orientation. The symbol located in the coordinate axis indicates that the ground motion is identified as non-pulse ground motion in the other directions.

5.3. Pseudo-velocity response spectrum

The response spectrum is widely applied in anti-seismic design. However, the effects of pulse on target spectra are insufficiently considered in anti-seismic codes. Hence, the response spectra of single- and multi-pulse ground motions are analyzed to facilitate the target spectra design in the near-fault regions. Besides, a comparative study between the period corresponding to the maximum value of 5% damped pseudo-spectral velocity and the pulse period identified by the proposed method is conducted to verify the feasibility of the response spectrum on pulse period estimation.

Examples of 5% damped pseudo-velocity response spectra of pulse-like ground motion are analyzed. The original, pulse, and residual ground motions of single- and multi-pulse ground motions are shown in Figure 9(a). The residual ground motion is the difference between the original ground motion and the extracted pulse. The pseudo-velocity response spectra of original, pulse, and residual ground motions are shown in Figure 9(b) and (c). It shows that the presence of pulses can dramatically magnify the peak value of the pseudo-velocity response spectrum. The spectrum becomes flat as the pulses are subtracted from the original ground motion. Besides, Figures 9(b) and (c) show that the pseudo-velocity response spectra of the multi-pulse ground motions generally contain multiple peaks. This phenomenon implies that the multi-pulse ground motion potentially causes severer damage to high-period structures than the single-pulse ground motion. Hence, the risk can be underestimated for the response spectrum-based seismic hazards analysis without considering the pulse part or only considering a single pulse.

The pulse periods determined by the pseudo-velocity response spectrum and the proposed method are compared based on the ground motions in Imperial Valley-06 and Chi-Chi Taiwan Earthquake. Results (see Figure 10) indicate that the spectrum-based periods mainly distribute in the range of $[-30\%, +30\%]$ of the pulse periods despite existing

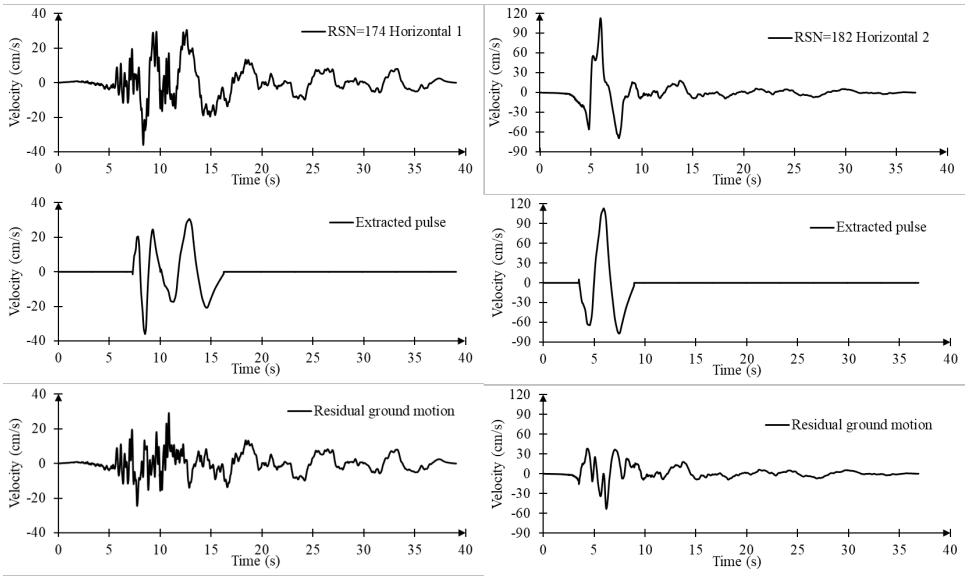

(a)

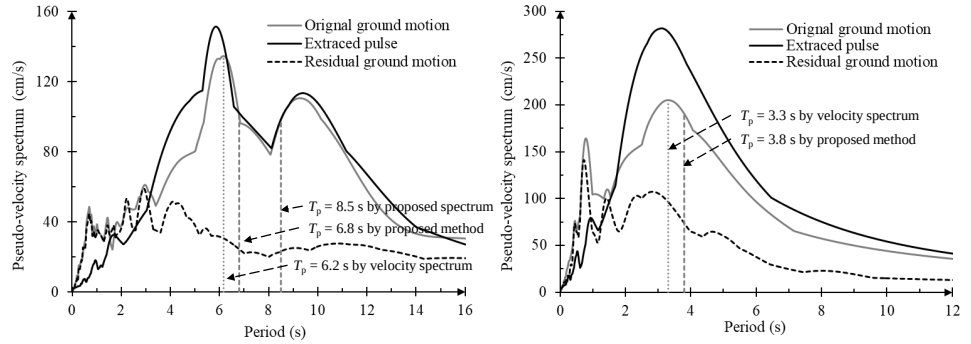

(b)

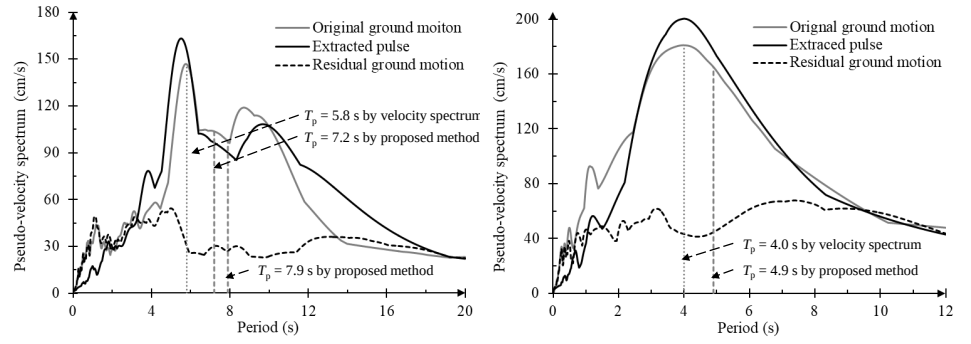

(c)

Figure 9: 5% damped spectral velocity of pulse-like ground motions. (a) The original, extracted pulse, and residual ground motion of multi-pulse (RSN 1493 Horizontal 2) and single-pulse (RSN 182 Horizontal 2) ground motion; (b) The spectral velocity of the ground motions in (a); (c) Other examples of the spectral velocity of multi- and single-pulse ground motion, where the left column is RSN 1499 Horizontal 2 and the right column is RSN 179 Horizontal 2.

outliers. Hence, the approximate estimations on the pulse period based on the pseudo-velocity response spectrum are a practical option for engineers, especially when the accuracy requirement is not strict.

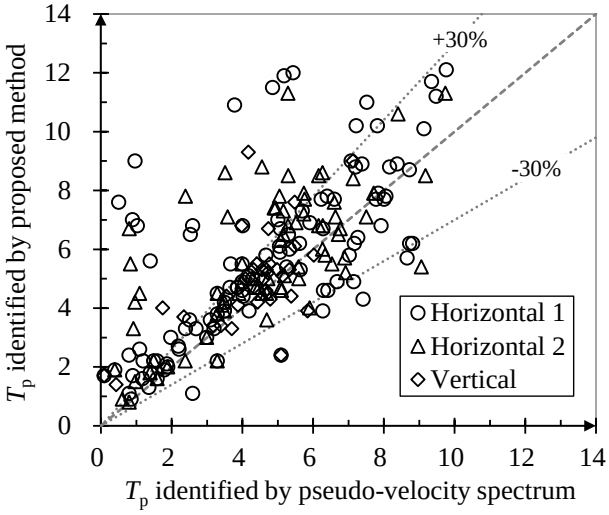

Figure 10: Comparison between the pulse period identified by the proposed method and the period corresponding to the maximum 5% damped pseudo-velocity response spectrum. The pulse-like ground motions in both the Imperial Valley-06 Earthquake and the Chi-Chi, Taiwan Earthquake databases are adopted.

However, the pulse period determination based on the pseudo-velocity response spectrum remains challenging. Firstly, accurate identification of the pulse period is difficult using the response spectrum. The spectrum-based period is generally less than the period identified by the proposed method, as shown in Figure 10. Secondly, only using the response spectrum cannot distinguish the ordinary and pulse-like ground motion. It is also challenging to discern the single- and multi-pulse ground motion. For example, although the multi-peak shape of the pseudo-velocity response spectrum can partially reflect the characteristics of the multi-pulse ground motions, the multiple peaks may also appear in the low period for the single-pulse ground motion, as shown in the right column of Figure 9(b).

6. Conclusions

A generalized continuous wavelet transform (GCWT) method is proposed by combining the convolution analysis and evaluation parameters for pulse-like ground motion identification. This method can effectively identify the single- and multi-pulse ground motions and overcomes the limitations of the classical CWT-based identification method that requires a wavelet basis. The proposed method requires each pulse in the identified multi-pulse ground motions to satisfy the same criteria and excludes the effects of the attenuation part that includes in other methods. The proposed procedure also provides a flexible and workable framework for pulse-like ground motion identification, which provides

the possibility for further studies, such as the effects of the pulse model on identification and the combination between signal processing technique and seismological mechanism.

The spectral velocity of multi-pulse ground motion potentially contains multiple peaks in the long-period range, which tends to cause severer damage to structures with a high fundamental period. Hence, the risk could be underestimated for the response spectrum-based seismic hazards and risk analysis when the multi-pulse features are not insufficiently considered. In addition, the period corresponding to the maximum spectral velocity can roughly estimate the pulse period of single-pulse ground motion. This study shows that while there are a few outliers, the spectrum-based pulse period can mainly distribute in the range of $[-30\%, +30\%]$ of the pulse periods identified by the proposed method.

Based on the proposed method, the pulse-like ground motions from the Imperial Valley-06 Earthquake and the Chi-Chi, Taiwan Earthquake in the PEER NGA-West2 database are identified and summarized in the Appendix to facilitate the wider studies on multi-pulse ground motions. The reliability of the proposed method is verified by a comparative study among the proposed, Baker's [13] and Zhai et al.'s [24] methods. To further facilitate the research on multi-pulse ground motions, case studies on seismic damage subjected to multi-pulse records will be carried out in future work.

Acknowledgements

This research is supported by the National Natural Science Foundation of China (Grant No. U22A20596) and the International Joint Research Platform Seed Fund Program of Wuhan University (Grant No. WHUZZJJ202207). Guan Chen would like to thank the financial support of Sino-German (CSC-DAAD) Postdoc Scholarship Program.

References

[1] George W Housner and Mihailo D Trifunac. Analysis of accelerograms—Parkfield earthquake. *Bulletin of the seismological society of America*, 57(6):1193–1220, 1967.

[2] Polsak Tothong and C Allin Cornell. Structural performance assessment under near-source pulse-like ground motions using advanced ground motion intensity measures. *Earthquake Engineering & Structural Dynamics*, 37(7):1013–1037, 2008.

[3] Guan Chen, Jiashu Yang, Yong Liu, Takeshi Kitahara, and Michael Beer. An energy-frequency parameter for earthquake ground motion intensity measure. *Earthquake Engineering & Structural Dynamics*, 2022.

[4] Guan Chen, Michael Beer, and Yong Liu. Modeling response spectrum compatible pulse-like ground motion. *Mechanical Systems and Signal Processing*, 177:109177, 2022.

[5] Eric M Dunham and Ralph J Archuleta. Near-source ground motion from steady state dynamic rupture pulses. *Geophysical Research Letters*, 32(3), 2005.

[6] Arben Pitarka, Kojiro Irikura, Tomotaka Iwata, and Haruko Sekiguchi. Three-dimensional simulation of the near-fault ground motion for the 1995 Hyogo-ken Nanbu (Kobe), Japan, earthquake. *Bulletin of the Seismological Society of America*, 88(2):428–440, 1998.

[7] Shih-Po Chang, Nicos Makris, Andrew S Whittaker, and Andrew CT Thompson. Experimental and analytical studies on the performance of hybrid isolation systems. *Earthquake Engineering & Structural Dynamics*, 31(2):421–443, 2002.

[8] Babak Alavi and Helmut Krawinkler. Behavior of moment-resisting frame structures subjected to near-fault ground motions. *Earthquake Engineering & Structural Dynamics*, 33(6):687–706, 2004.

[9] Shuai Li, Fan Zhang, Jing-quan Wang, M Shahria Alam, and Jian Zhang. Effects of near-fault motions and artificial pulse-type ground motions on super-span cable-stayed bridge systems. *Journal of Bridge Engineering*, 22(3):04016128, 2017.

[10] Yuan Lu and Marios Panagiotou. Characterization and representation of near-fault ground motions using cumulative pulse extraction with wavelet analysis. *Bulletin of the Seismological Society of America*, 104(1):410–426, 2014.

[11] Xiaoyu Chen, Dongsheng Wang, and Rui Zhang. Identification of pulse periods in near-fault ground motions using the HHT method. *Bulletin of the Seismological Society of America*, 109(6):2384–2398, 2019.

[12] Xiaoyu Chen and Dongsheng Wang. Multi-pulse characteristics of near-fault ground motions. *Soil Dynamics and Earthquake Engineering*, 137:106275, 2020.

[13] Jack W Baker. Quantitative classification of near-fault ground motions using wavelet analysis. *Bulletin of the Seismological Society of America*, 97(5):1486–1501, 2007.

[14] George P Mavroeidis and Apostolos S Papageorgiou. A mathematical representation of near-fault ground motions. *Bulletin of the Seismological Society of America*, 93(3):1099–1131, 2003.

[15] Jonathan D Bray and Adrian Rodriguez-Marek. Characterization of forward-directivity ground motions in the near-fault region. *Soil Dynamics and Earthquake Engineering*, 24(11):815–828, 2004.

[16] Reeves Whitney. Quantifying near fault pulses using generalized morse wavelets. *Journal of Seismology*, 23(5):1115–1140, 2019.

[17] Bryce W Dickinson and Henri P Gavin. Parametric statistical generalization of uniform-hazard earthquake ground motions. *Journal of Structural Engineering*, 137(3):410–422, 2011.

[18] Guan Chen, Qi-Yue Li, Dian-Qing Li, Zheng-Yu Wu, and Yong Liu. Main frequency band of blast vibration signal based on wavelet packet transform. *Applied Mathematical Modelling*, 74:569–585, 2019.

[19] Changhai Zhai, Cuihua Li, Sashi Kunnath, and Weiping Wen. An efficient algorithm for identifying pulse-like ground motions based on significant velocity half-cycles. *Earthquake Engineering & Structural Dynamics*, 47(3):757–771, 2018.

[20] Ping Liu, Ning Li, Hua Ma, Lili Xie, and Baofeng Zhou. Relative energy zero ratio-based approach for identifying pulse-like ground motions. *Earthquake Engineering and Engineering Vibration*, 19(1):1–16, 2020.

[21] Guochen Zhao, Longjun Xu, and Lili Xie. A simple and quantitative algorithm for identifying pulse-like ground motions based on zero velocity point method. *Bulletin of the Seismological Society of America*, 106(3):1011–1023, 2016.

[22] Petros Mimoglou, Ioannis N Psycharis, and Ioannis M Taflampas. Explicit determination of the pulse inherent in pulse-like ground motions. *Earthquake Engineering & Structural Dynamics*, 43(15):2261–2281, 2014.

[23] Suparno Mukhopadhyay and Vinay K Gupta. Directivity pulses in near-fault ground motions—I: Identification, extraction and modeling. *Soil Dynamics and Earthquake Engineering*, 50:1–15, 2013.

[24] Changhai Zhai, Zhiwang Chang, Shuang Li, ZhiQiang Chen, and Lili Xie. Quantitative identification of near-fault pulse-like ground motions based on energy. *Bulletin of the Seismological Society of America*, 103(5):2591–2603, 2013.

[25] Chin-Hsiung Loh, Tsu-Chiu Wu, and Norden E Huang. Application of the empirical mode decomposition-hilbert spectrum method to identify near-fault ground-motion characteristics and structural responses. *Bulletin of the Seismological Society of America*, 91(5):1339–1357, 2001.

[26] Praveen K Malhotra. Response of buildings to near-field pulse-like ground motions. *Earthquake Engineering & Structural Dynamics*, 28(11):1309–1326, 1999.

[27] R Rupakhety, SU Sigurdsson, AS Papageorgiou, and R Sigbjörnsson. Quantification of ground-motion parameters and response spectra in the near-fault region. *Bulletin of Earthquake Engineering*, 9(4):893–930, 2011.

[28] Guan Chen, Kaiqi Li, and Yong Liu. Applicability of continuous, stationary, and discrete wavelet transforms in engineering signal processing. *Journal of Performance of Constructed Facilities*, 35(5):04021060, 2021.

[29] Dixiong Yang and Jilei Zhou. A stochastic model and synthesis for near-fault impulsive ground motions. *Earthquake Engineering & Structural Dynamics*, 44(2):243–264, 2015.

[30] A Plešinger, M Hellweg, and D Seidl. Interactive high-resolution polarization analysis of broad-band seismograms. *Journal of Geophysics*, 59(1):129–139, 1986.

[31] Antonio Scala, G Festa, and S Del Gaudio. Relation between near-fault ground motion impulsive signals and source parameters. *Journal of Geophysical Research: Solid Earth*, 123(9):7707–7721, 2018.

[32] Suparno Mukhopadhyay and Vinay K Gupta. Directivity pulses in near-fault ground motions—II: Estimation of pulse parameters. *Soil Dynamics and Earthquake Engineering*, 50:38–52, 2013.

[33] Paul G Somerville, Nancy F Smith, Robert W Graves, and Norman A Abrahamson. Modification of empirical strong ground motion attenuation relations to include the amplitude and duration effects of rupture directivity. *Seismological Research Letters*, 68(1):199–222, 1997.

[34] Paul Spudich, Badie Rowshandel, Shrey K Shahi, Jack W Baker, and Brian S-J Chiou. Comparison of NGA-West2 directivity models. *Earthquake Spectra*, 30(3):1199–1221, 2014.

[35] Mayssa Dabaghi and Armen Der Kiureghian. Simulation of orthogonal horizontal components of near-fault ground motion for specified earthquake source and site characteristics. *Earthquake Engineering & Structural Dynamics*, 47(6):1369–1393, 2018.

[36] Mayssa Dabaghi and Armen Der Kiureghian. Stochastic model for simulation of near-fault ground motions. *Earthquake Engineering & Structural Dynamics*, 46(6):963–984, 2017.

[37] Hiroshi Kawase. The cause of the damage belt in Kobe:"The basin-edge effect," constructive interference of the direct S-wave with the basin-induced diffracted/Rayleigh waves. *Seismological Research Letters*, 67(5):25–34, 1996.

Appendix: Summary of identified pulse-like ground motions based on proposed method

The identified pulse-like ground motions of Imperial Valley-06 Earthquake and the Chi-Chi, Taiwan Earthquake in PEER NGA-West2 database and the corresponding parameters are summarized in Table 3. The corresponding pulse periods of Baker's and Zhai et al.'s study are also collected. Limited by space, only the originally recorded ground motions are listed in Table 3. The rotated fault-normal and fault-parallel ground motions are summarized in Supporting information in Table S1.

Table 3: The parameters of identified pulse-like ground motions.†

RSN	T_B	T_Z	Horizontal 1 (H1)				Horizontal 2 (H2)				Vertical (V)				M
			T_p	PGV	E_r	ρ	T_p	PGV	E_r	ρ	T_p	PGV	E_r	ρ	
Earthquake Name: Imperial Valley-06															
158	2.4	1.8	2.2	42.8	0.54	0.96	-	-	-	-	-	-	-	-	-
159	2.3	1.8	2.2	34.9	0.69	0.93	2.0	41.7	0.65	0.97	-	-	-	-	-
160	-	-	2.4	39.8	0.48	0.76	-	-	-	-	-	-	-	-	-
161	4.0	3.2	3.6	36.6	0.64	0.88	1.6	40.9	0.48	0.87	-	-	-	-	-
170	4.5	3.9	5.6	38.4	0.69	0.63	2.2	73.4	0.55	0.86	-	-	-	-	-
171	3.3	2.7	1.1	72.9	0.52	0.93	3.0	92.6	0.83	0.98	-	-	-	-	-
173	4.5	3.3	4.6	50.7	0.66	0.86	2.2	46.4	0.55	0.87	-	-	-	-	-
174	7.4	0.5	4.3	30.6	0.47	0.89	1.9	44.6	0.40	0.83	-	-	-	-	-
178	5.2	4.2	2.7	48.0	0.63	0.92	5.0	43.3	0.78	0.96	-	-	-	-	-
179	4.6	3.3	7.0	39.6	0.78	0.60	4.9	78.0	0.57	0.63	-	-	-	-	-
180	4.0	3.8	3.3	48.9	0.42	0.83	4.2	96.9	0.88	0.90	2.4	39.5	0.50	0.87	-
181	3.8	3.5	3.3	58.4	0.35	0.87	3.9	113.5	0.92	0.93	1.7	63.5	0.61	0.76	-
182	4.2	3.4	2.6	51.7	0.63	0.86	3.8	113.1	0.93	0.94	-	-	-	-	-
183	5.4	4.2	-	-	-	-	5.5	52.1	0.9	0.83	-	-	-	-	-
184	5.9	3.8	6.8	75.5	0.89	0.77	1.8	40.9	0.34	0.81	-	-	-	-	-
185	4.8	4.2	4.6	53.1	0.86	0.94	4.5	51.4	0.71	0.91	-	-	-	-	-
Earthquake Name: Chi-Chi, Taiwan															
1180	-	-	-	-	-	-	7.1	56.2	0.49	0.9	-	-	-	-	-
1182	2.6	2.2	2.1	60.2	0.52	0.74	-	-	-	-	-	-	-	-	-
1183	-	-	4.7	31.1	0.32	0.96	-	-	-	-	-	-	-	-	-
1193	-	-	4.4	51.1	0.5	0.86	4.6	43.5	0.48	0.94	4.3	47.3	0.43	0.92	-
1194	-	-	-	-	-	-	7.7	30.5	0.46	0.66	6.8	34.3	0.34	0.81	-
1195	-	-	5.9	40.9	0.37	0.96	-	-	-	-	-	-	-	-	-
1197	-	-	-	-	-	-	0.8	55	0.43	0.74	4.0	31.0	0.62	0.75	-
1198	-	-	-	-	-	-	4.0	39.7	0.36	0.87	-	-	-	-	-
1202	1.4	1.4	1.3	43.6	0.47	0.97	-	-	-	-	-	-	-	-	-

Continued on next page

Continuing Table 3

RSN	T_B	T_Z	Horizontal 1 (H1)				Horizontal 2 (H2)				Vertical (V)				M
			T_p	PGV	E_r	ρ	T_p	PGV	E_r	ρ	T_p	PGV	E_r	ρ	
1203	-	-	-	-	-	-	5.8	40.2	0.39	0.85					-
1231	-	-	0.9	106.8	0.38	0.94	1.5	84.4	0.33	0.94	1.4	41.0	0.4	0.79	-
1238	-	-	4.7	53.2	0.35	0.93	-	-	-	-	-	-	-	-	-
1244	4.8	3.9	3.3	65.0	0.46	0.93	5.0	109	0.72	0.93	-	-	-	-	-
1246	-	-	-	-	-	-	7.4	52.6	0.42	0.72	4.2	33.1	0.4	0.97	-
1329	-	-	-	-	-	-	-	-	-	-	-	-	-	-	-
1342	-	-	-	-	-	-	-	-	-	-	-	-	-	-	-
1343	-	-	-	-	-	-	5.1	31.0	0.36	0.92	-	-	-	-	-
1402	-	-	-	-	-	-	-	-	-	-	-	-	-	-	-
1410	3.4	3.0	-	-	-	-	-	-	-	-	-	-	-	-	-
1454	-	-	1.6	32.4	0.32	0.92	-	-	-	-	-	-	-	-	-
1463	-	-	7.8	34.9	0.38	0.92	-	-	-	-	-	-	-	-	-
1464	-	-	9.0	33.9	0.63	0.89	-	-	-	-	-	-	-	-	-
1467	-	-	10.2	30.2	0.61	0.80	-	-	-	-	-	-	-	-	-
1468	-	-	11.0	33.2	0.43	0.81	-	-	-	-	-	-	-	-	-
1471	-	-	7.7	41.8	0.64	0.92	-	-	-	-	-	-	-	-	-
1472	-	-	6.2	36.7	0.54	0.88	7.6	34.4	0.64	0.85	-	-	-	-	-
1473	-	-	8.9	37.8	0.69	0.89	-	-	-	-	-	-	-	-	-
1475	-	-	6.2	37.9	0.58	0.87	-	-	-	-	-	-	-	-	-
1476	6.4	5.4	7.7	37.5	0.59	0.91	4.7	51.9	0.68	0.92	-	-	-	-	-
1477	6.2	5.1	6.1	53.9	0.69	0.96	-	-	-	-	-	-	-	-	-
1478	-	-	6.7	41.5	0.6	0.90	-	-	-	-	-	-	-	-	-
1479	8.6	7.2	6.2	43.6	0.58	0.87	-	-	-	-	-	-	-	-	-
1480	5.4	5.7	6.5	57.5	0.72	0.95	-	-	-	-	-	-	-	-	-
1481	7.0	5.9	6.9	56.7	0.66	0.92	6.8	38.8	0.62	0.89	5.3	32.3	0.8	0.94	-
1482	-	-	4.9	54.8	0.31	0.86	5.4	56.6	0.72	0.91	5.3	50.4	0.8	0.91	-
1483	6.3	5.7	6.2	56.8	0.76	0.96	-	-	-	-	-	-	-	-	-
1484	9.1	7.0	8.8	30.8	0.31	0.87	4.5	36.2	0.34	0.89	-	-	-	-	-

Continued on next page

Continuing Table 3

RSN	T_B	T_Z	Horizontal 1 (H1)				Horizontal 2 (H2)				Vertical (V)				M
			T_p	PGV	E_r	ρ	T_p	PGV	E_r	ρ	T_p	PGV	E_r	ρ	
1485	-	-	-	-	-	-	0.9	46.4	0.32	0.96	-	-	-	-	-
1486	8.6	7.1	-	-	-	-	-	-	-	-	5.0	32.4	0.76	0.88	-
1487	-	-	9.0	42.0	0.86	0.76	-	-	-	-	-	-	-	-	-
1488	-	-	10.9	34.3	0.49	0.77	7.4	47.3	0.48	0.94	-	-	-	-	-
1489	11.8	1.1	10.1	53.5	0.8	0.87	8.6 6.0	41.1 62.3	0.43 0.45	0.92 0.92	-	-	-	-	Y
1490	-	-	11.2	36.7	0.67	0.85	8.5	43.3	0.48	0.90	5.1	42.1	0.63	0.98	-
1491	-	-	4.9	53.8	0.45	0.8	8.4	41.7	0.55	0.94	-	-	-	-	-
1492	-	-	7.3	151.1	0.92	0.9	11.3	172	0.89	0.91	9.0	144	0.95	0.96	-
1493	12.9	1.5	12.1	39.6	0.79	0.86	8.5 6.8	38.9 46.3	0.50 0.39	0.95 0.95	3.9	32.5	0.4	0.88	Y
1494	1.5	8.4	-	-	-	-	8.5	32.4	0.4	0.91	7.6	30.1	0.47	0.73	-
1495	-	-	-	-	-	-	8.8 4.5	34.8 48.9	0.41 0.34	0.90 0.92	5.3	59.1	0.65	0.9	Y
1496	12.9	4.7	4.3	33.9	0.38	0.68	7.9	39.5	0.55	0.88	4.4	41.8	0.43	0.89	-
1497	-	-	11.9	38.2	0.62	0.79	7.1	49.3	0.52	0.93	5.3	33.9	0.56	0.90	-
1498	-	-	4.6	51.4	0.37	0.86	11.3 6.8	49.5 53.5	0.42 0.44	0.68 0.88	-	-	-	-	Y
1499	12.0	11.9	-	-	-	-	7.9 7.2	41.0 44.0	0.44 0.46	0.93 0.90	-	-	-	-	Y
1500	-	-	5.3	40.8	0.4	0.91	7.1	36.7	0.32	0.9	-	-	-	-	-
1501	-	-	6.0	44.0	0.42	0.91	4.7	82.8	0.57	0.96	4.6	57.0	0.55	0.91	-
1502	-	-	5.8	42.7	0.45	0.86	6.7	55.3	0.5	0.95	3.4	32.2	0.31	0.98	-
1503	5.7	4.8	5.8	109.6	0.32	0.91	-	-	-	-	3.3	68.9	0.38	0.81	-
1504	-	-	2.6	92.0	0.48	0.82	-	-	-	-	4.5	49.8	0.48	0.92	-
1505	12.2	8.1	11.7	249.5	0.96	0.89	10.6	264	0.96	0.96	9.3	213	0.96	0.90	-
1506	-	-	6.7	37.2	0.48	0.70	6.3 4.7	56.2 60.2	0.34 0.38	0.91 0.88	5.3	36.2	0.48	0.95	Y

Continued on next page

Continuing Table 3

RSN	T_B	T_Z	Horizontal 1 (H1)				Horizontal 2 (H2)				Vertical (V)				M
			T_p	PGV	E_r	ρ	T_p	PGV	E_r	ρ	T_p	PGV	E_r	ρ	
1507	-	-	-	-	-	-	4.2	39.7	0.42	0.76	5.8	38	0.48	0.91	-
1508	-	-	-	-	-	-	-	-	-	-	-	-	-	-	-
1509	-	-	-	-	-	-	-	-	-	-	-	-	-	-	-
1510	5.1	4.0	5.1	109.5	0.76	0.92	5.2	36.1	0.36	0.9	3.4	50.9	0.47	0.97	-
1511	4.0	3.3	3.9	51.8	0.52	0.91	5.5	59.7	0.51	0.72	-	-	-	-	-
1514	-	-	7.8	39.0	0.59	0.86	-	-	-	-	-	-	-	-	-
1515	9.2	8	3.9	54.9	0.37	0.71	8.6	38.1	0.48	0.9	6.1	34.9	0.56	0.83	-
1516	-	-	10.2	30.1	0.50	0.91	-	-	-	-	-	-	-	-	-
1517	-	-	1.7	128.8	0.33	0.94	3.3	48.1	0.32	0.69	-	-	-	-	-
1519	9.0	5.3	8.7	45.0	0.70	0.90	4.5	40.5	0.65	0.96	5.5	58.4	0.90	0.90	-
1521	-	-	-	-	-	-	4.5	32.0	0.38	0.79	-	-	-	-	-
1523	-	-	5.7	38.8	0.49	0.90	-	-	-	-	-	-	-	-	-
1524	-	-	-	-	-	-	-	-	-	-	-	-	-	-	-
1525	-	-	7.9	38.1	0.66	0.88	-	-	-	-	-	-	-	-	-
1526	7.5	6.3	7.7	45.6	0.60	0.91	-	-	-	-	-	-	-	-	-
1506	-	-	11.5	38.0	0.60	0.83	6.5 7.3	35.7 42.9	0.36 0.41	0.94 0.89	5.0	39.5	0.68	0.90	Y
1528	1.0	5.6	8.8	76.8	0.84	0.89	5.0	51.0	0.46	0.89	5.0	46.7	0.76	0.93	-
1529	9.7	4.3	3.6	91.7	0.58	0.78	2.2	66.4	0.41	0.71	3.7	68.4	0.66	0.94	-
1530	8.3	6.4	6.4	70.2	0.69	0.92	-	-	-	-	6.7	60.9	0.82	0.88	-
1531	12.0	8.3	12.0	30.4	0.35	0.88	6.9	47.5	0.5	0.98	-	-	-	-	-
1532	-	-	7.0	33.0	0.45	0.96	5.4	35.8	0.36	0.69	-	-	-	-	-
1533	-	-	-	-	-	-	7.8	31.3	0.33	0.93	-	-	-	-	-
1534	-	-	7.7	34.2	0.37	0.90	7.8	40.9	0.33	0.77	-	-	-	-	-
1535	-	-	6.5	56.9	0.46	0.88	4.1	56.4	0.36	0.91	-	-	-	-	-
1537	-	-	5.5	53.3	0.42	0.94	-	-	-	-	-	-	-	-	-
1538	-	-	-	-	-	-	-	-	-	-	-	-	-	-	-
1540	-	-	4.7	48.7	0.47	0.95	-	-	-	-	-	-	-	-	-

Continued on next page

Continuing Table 3

RSN	T_B	T_Z	Horizontal 1 (H1)				Horizontal 2 (H2)				Vertical (V)				M
			T_p	PGV	E_r	ρ	T_p	PGV	E_r	ρ	T_p	PGV	E_r	ρ	
1541	-	-	6.8	42.1	0.51	0.76	-	-	-	-	5.2	34.1	0.34	0.90	-
1542	-	-	-	-	-	-	-	-	-	-	-	-	-	-	-
1545	-	-	3.0	59.8	0.38	0.86	5.7	34.6	0.38	0.85	4.4	35.3	0.38	0.78	-
1546	-	-	6.8	42.1	0.43	0.84	6.5	43.5	0.46	0.83	-	-	-	-	-
1547	-	-	-	-	-	-	-	-	-	-	-	-	-	-	-
1548	9.0	5.1	6.8	63.7	0.66	0.88	3.6	62.6	0.53	0.87	4.1	44.9	0.54	0.95	-
1549	-	-	7.6	62.8	0.66	0.81	6.7	52.9	0.44	0.77	5.5	38.8	0.36	0.82	-
1550	1.3	8.6	8.9	45.4	0.73	0.96	5.5	51.4	0.55	0.92	4.7	33.3	0.57	0.82	-
1551	-	-	-	-	-	-	-	-	-	-	-	-	-	-	-
1553	-	-	5.4	45.8	0.43	0.94	-	-	-	-	-	-	-	-	-

† RSN - 'Record Sequence Number' in PEER NGA-West2 flatfile; T_B - The pulse period from Baker's study [13]; T_Z- The pulse period from Zhai el al.'s study [24]; Horizontal 1 / Horizontal 2 / Vertical - The direction defined in PEER NGA-West2 flatfile; T_p - The pulse period identified by the proposed method; PGV - Peak Ground Velocity of the recorded pulse part (i.e. the identified pulse part of the original ground motion); E_r - the energy ratio between the recorded pulse part and the original ground motion; ρ - Pearson correlation coefficient between the recorded pulse part and the pulse model; M - Whether the ground motions contain multi-pulses, and 'Y' denotes contains multiple pulses; The parameters of the proposed method for the results in this table are listed in Table 2.